SCIENTIFIC REPORTS

OPEN

Morphological changes in response to environmental stresses in the fungal plant pathogen *Zymoseptoria tritici*

Received: 11 November 2018
Accepted: 20 June 2019
Published online: 03 July 2019

Carolina Sardinha Francisco, Xin Ma, Maria Manuela Zwyssig, Bruce A. McDonald & Javier Palma-Guerrero

During their life cycles, pathogens have to adapt to many biotic and abiotic environmental stresses to maximize their overall fitness. Morphological transitions are one of the least understood of the many strategies employed by fungal plant pathogens to adapt to constantly changing environments, even though different morphotypes may play important biological roles. Here, we first show that blastospores (the "yeast-like" form of the pathogen typically known only under laboratory conditions) can form from germinated pycnidiospores (asexual spores) on the surface of wheat leaves, suggesting that this morphotype can play an important role in the natural history of *Z. tritici*. Next, we characterized the morphological responses of this fungus to a series of environmental stresses to understand the effects of changing environments on fungal morphology and adaptation. All tested stresses induced morphological changes, but different responses were found among four strains. We discovered that *Z. tritici* forms chlamydospores and demonstrated that these structures are better able to survive extreme cold, heat and drought than other cell types. Finally, a transcriptomic analysis showed that morphogenesis and the expression of virulence factors are co-regulated in this pathogen. Our findings illustrate how changing environmental conditions can affect cellular morphology and lead to the formation of new morphotypes, with each morphotype having a potential impact on both pathogen survival and disease epidemiology.

Fungi occupy a wide range of niches that can impose different environmental constraints on their growth, reproduction and survival. In response, fungi evolved the ability to detect and respond to different environmental stimuli to maximize their fitness[1]. One of the strategies that fungi employ to cope with diverse biotic and abiotic stresses is to change their morphology[2–4]. For fungal pathogens, different morphotypes can play different roles during the host-pathogen interaction to optimize overall pathogen fitness. For example, hyphae can be the most appropriate morphology to cross physical barriers, colonize host tissue[2,5], and escape harmful environments generated by host defences[2,6] while yeast cells (or "yeast-like" cells) may be a better morphology to enable dispersal among host niches or between hosts and increase the pathogen population size[2,7]. The majority of fungal morphotype transitions occur between hyphal and yeast growth forms. Fungi with this ability are called dimorphic. Usually, they grow as saprotrophic molds that live on dead organic matter and many are facultative human pathogens, though dimorphism is also found in plant pathogens[2,8,9]. The morphological transition can be co-regulated with the expression of genes encoding virulence[2–5,7,10–12]. For the well-studied dimorphic plant pathogen *Ustilago maydis*, the causal agent of corn smut, both filamentation and virulence are co-regulated by a complex network of intracellular signalling pathways[12,13]. The induction of virulence genes can be associated with a specific morphotype. For example, certain virulence genes are expressed only during the yeast-phase of growth in *Histoplasma capsulatum*, while other virulence genes are expressed only during hyphal growth in *Candida albicans*[5,6,14].

Some fungi can produce additional morphologies, including pseudohyphae and chlamydospores. These fungi that alternate through multiple morphotypes are called pleomorphic. Pseudohyphae are distinguished from true hyphae by constrictions that form at the septal junctions, leading to a loss in cytoplasmic continuity between

Plant Pathology Group, Institute of Integrative Biology, ETH Zürich, 8092, Zürich, Switzerland. Correspondence and requests for materials should be addressed to C.S.F. (email: carolina.sardinha@usys.ethz.ch) or J.P.-G. (email: javier.palma@usys.ethz.ch)

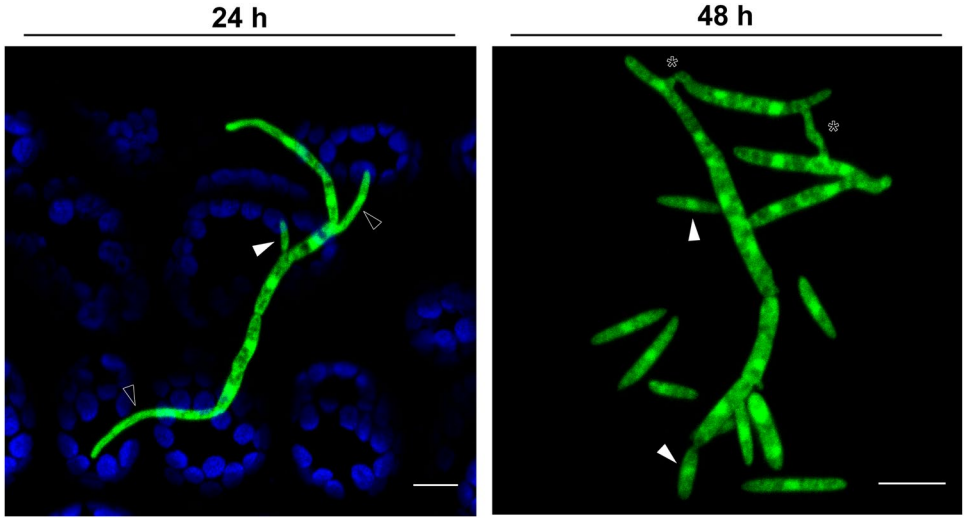

Figure 1. Germinated pycnidiospores of *Zymoseptoria tritici* produce new blastospores via blastosporulation on the surface of wheat leaves. At 24 hours after infection, pycnidiospores germinated and formed hyphal branches expressing GFP (green color). The germinated pycnidiospores produced new blastospores (white triangles) on the host leaves. We observed a significant increase of budding points on germinated pycnidiospores, as well as more free blastospores on the leaf surface at 48 hours after infection. At this time point, we also observed several vegetative cell fusion events between blastospores and pycnidiospores, which are characterized by a tubular shaped bridge between the fusing cells (asterisks). Blue color corresponds to autofluorescence detected from Chlorophyll A. Bars represent 10 μm.

mother and daughter cells[15]. Though little is known about the ecological significance of pseudohyphae and their role during host infection, it was suggested that this morphotype facilitates foraging for scarce nutrients and increases motility in the host, as well as the cell-to-cell movement observed in *Magnaporthe oryzae*[7,16,17]. Chlamydospores are spherical, thick-walled cells formed on the tips of pseudohyphae or on distal parts of differentiated hyphae called suspensor cells[18]. In contrast to pseudohyphae, chlamydospores are well-characterized and known to operate as long-term survival structures that can resist many environmental stresses[18–22]. Pleomorphism has been observed in fungal pathogens of humans[18,20,23] and plants[21,24,25].

Zymoseptoria tritici is the most damaging pathogen of wheat in Europe[26,27] and an important pathogen of wheat worldwide. *Z. tritici* is considered a dimorphic fungus that grows either as blastospores (the "yeast-like" form) or as filamentous hyphae depending on the culture conditions. Though the role of blastospores in nature was unclear until now, hyphae formed from either germinated ascospores (sexual spores) or pycnidiospores (asexual spores) are essential for penetrating wheat leaves through stomata[28,29]. The stimuli that induce morphological changes and the cell signaling pathways involved in morphological transitions remain largely unknown in this pathogen. Nutrient-rich media and temperatures ranging from 15 °C to 18 °C tend to induce blastosporulation (blastospore replication by budding) while nutrient-limited media and high temperatures (from 25 °C to 28 °C) tend to promote the blastospore-to-hyphae transition in the *Z. tritici* reference strain IPO323[30,31]. Some genes affecting morphogenesis in *Z. tritici* were identified and functionally characterized. Most of these belonged to the mitogen-activated protein kinase (MAPK) or cAMP-dependent signaling pathways involved in extracellular signal transduction, regulating many cellular processes, development and virulence[30–40]. However, the transcriptome signatures associated with specific morphotypes were not reported until now.

In this study we aimed to determine whether morphological changes allow *Z. tritici* to tolerate different environmental stresses and whether the different morphotypes play important biological roles. We showed that blastospores can form by budding from pycnidiospores inoculated onto the surface of wheat leaves, demonstrating that blastospores can be produced under natural conditions. We found that *Z. tritici* changed its morphology in response to all tested stresses, though distinct responses were observed for four strains sampled from the same geographical population. We discovered that *Z. tritici* forms chlamydospores both *in vitro* and *in planta*. We also found that pseudohyphae will form in some environments. Transcriptional analyses showed co-regulation of mycelial growth and virulence factors. Based on these findings, we propose that morphological transitions in *Z. tritici* are a stress response that allows the fungus to optimize fitness in a changing environment.

Results

Germinating pycnidiospores produce blastospores on the surface of wheat leaves. To investigate the production of blastospores in nature, we inoculated pycnidiospores of a GFP-tagged 3D7 strain onto wheat plants and monitored them by confocal microscopy. At 24 hours post infection (hpi), we observed the expected pycnidiospore germination and initial hyphal branching (Fig. 1, open triangles), but we also observed newly-budding blastospores (white triangles). After 48 hours, there was an increase in the number of budding points on germinated pycnidiospores, and an increase in the number of free blastospores visible on the leaf (white arrows). This suggests that pycnidiospores of *Z. tritici* can germinate to produce additional blastospores

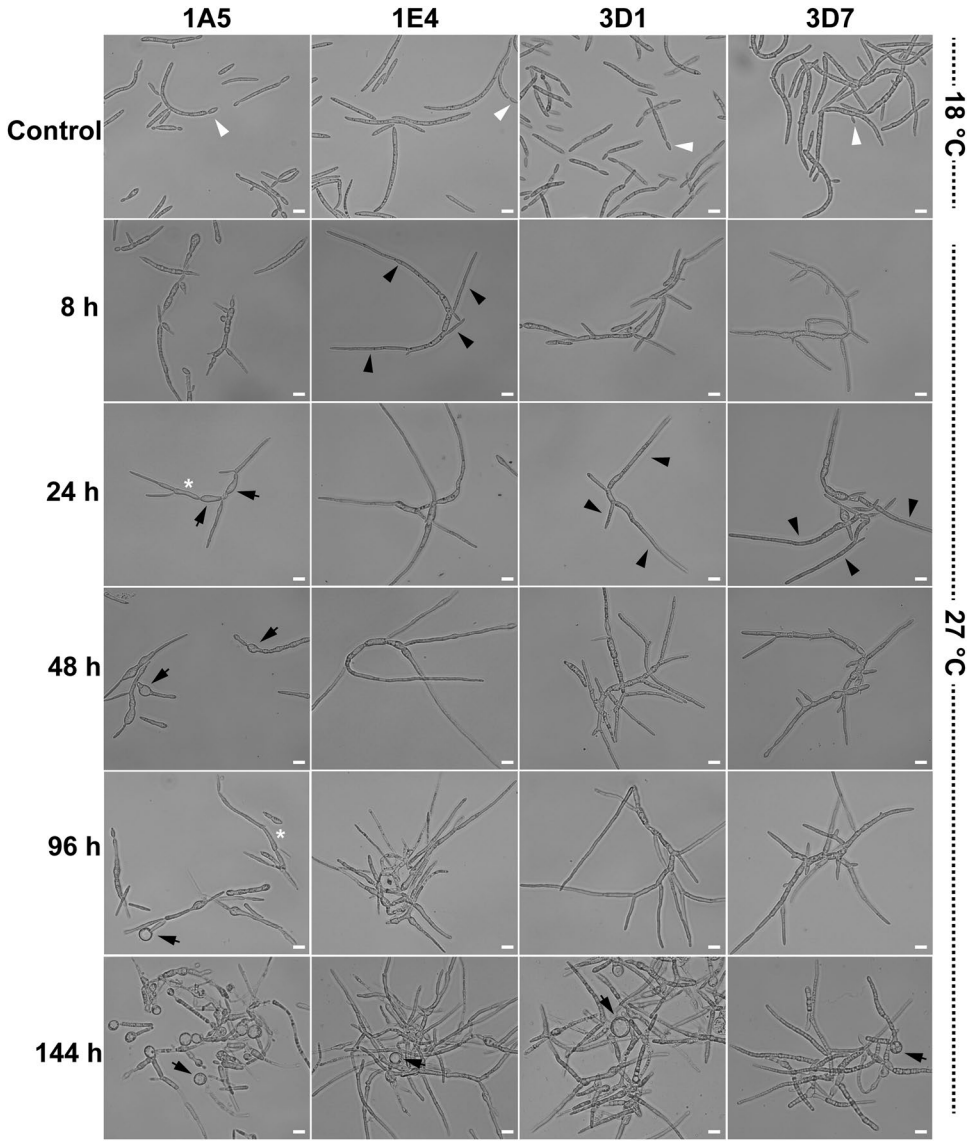

Figure 2. Effect of temperature on the cell morphology of four *Zymoseptoria tritici* strains. Blastospores incubated on nutrient-rich YSB medium at 18 °C (the control environment) multiply by budding as blastospores (white triangles). The effect of high temperatures on *Z. tritici* morphology was observed by exposing the strains to 27 °C. At 8 hours after incubation (hai) at the high temperature, blastospores of the 1E4 strain were faster to respond to the new environment by switching to filamentous growth. At 24 hai, blastospores of the 3D1 and 3D7 strains began growing as hyphae. Black triangles point to hyphal branches. The 1A5 strain produced swollen cells (black arrows) and pseudohyphae (white asterisk), without any evidence of hyphal differentiation. At 48 hai, hyphal branches were abundant for the 1E4, 3D1, and 3D7 strains. The 1A5 strain continued to produce only swollen structures. At 96 hai, filamentous growth was observed for the 1E4, 3D1, and 3D7 strains. For the 1A5 strain, high temperature promoted the formation of two new morphotypes: pseudohyphae (white asterisk) and chlamydospore-like cells (black arrows). After 144 hours of incubation, the formation of chlamydospore-like cells was observed mainly at the tips of pseudohyphae for the 1A5 strain and at the distal ends of mycelial filaments for the remaining strains (1E4, 3D1, and 3D7). Bars represent 10 µm.

even before penetration of the wheat leaf, providing an alternative mechanism for splash dispersal of infective propagules and potentially providing a substantial increase in the total inoculum load associated with an infection cycle. At 48 hpi we also noticed many anastomosis events between pycnidiospores and new blastospores (asterisks).

High temperature induces different morphological responses among *Z. tritici* strains. The effect of heat stress on morphological transitions was assessed by exposing four *Z. tritici* strains growing in yeast sucrose broth (YSB) to 27 °C, a highly stressful temperature for *Z. tritici*. Three of the strains (1E4, 3D1, and 3D7) differentiated to filamentous growth at 27 °C (Fig. 2, black triangles) as previously reported for the reference strain IPO323[30,31]. The timing of the hyphal transition ranged from 8 hours after incubation (hai) for 1E4, to 24 hai for

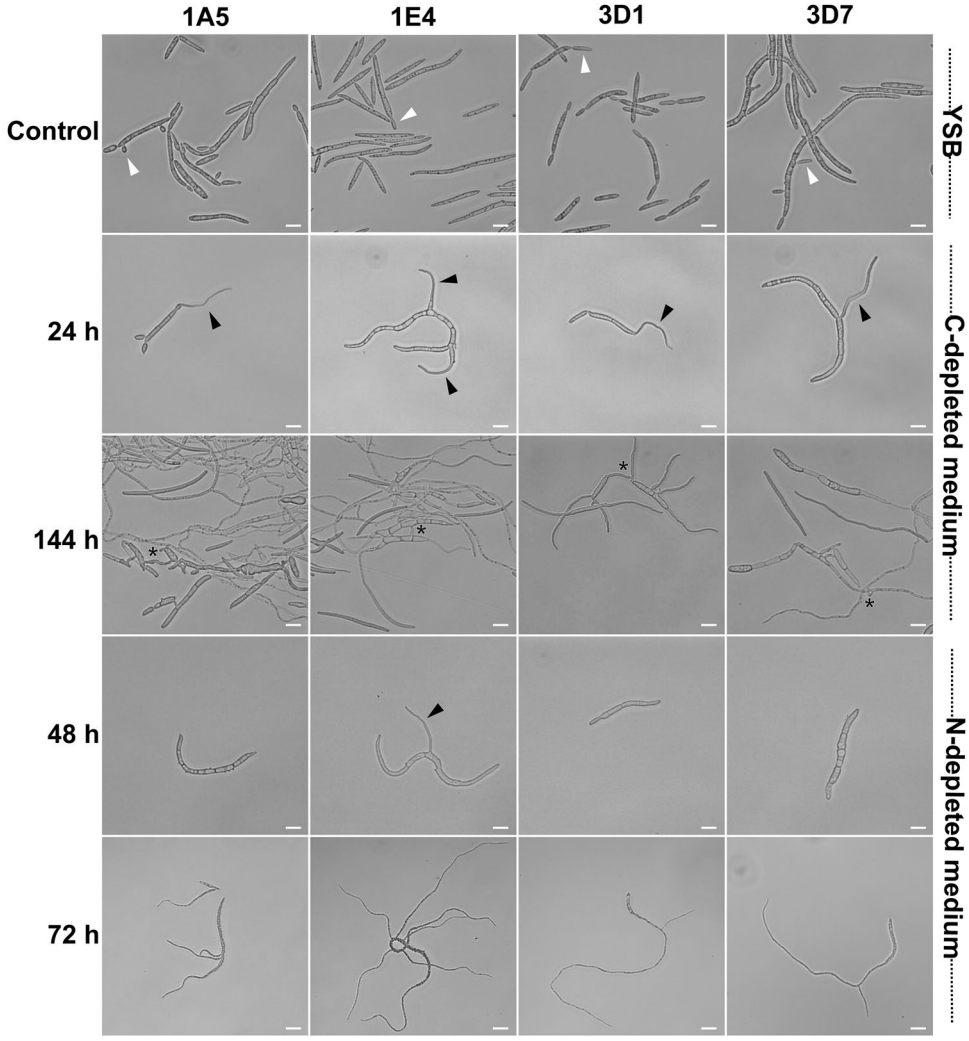

Figure 3. Effect of carbon and nitrogen limitation on the cell morphology of four *Zymoseptoria tritici* strains. Liquid media with distinct nutritional contents were used to monitor the growth form transitions. Blastospores incubated on nutrient-rich medium (YSB) continued to multiply as budding blastospores (white triangles) and were used as controls. Under C-depleted stress (Minimal Media without sucrose), the blastospores of all tested strains began growing as hyphae after 24 hours of incubation (black triangles). At 144 hai, a mycelial growth was predominant, with frequent vegetative cell fusion events (asterisks) among hyphae. Bars represent 10 µm. At 48 hai under N-depleted stress (MM without ammonium nitrate), only blastospores from the 1E4 strain switched to hyphal growth forming lateral filaments. The rest of the strains remain undifferentiated. Bars represent 10 µm. At 72 hai, blastospores of all tested *Z. tritici* strains incubated under nitrogen depletion undergo a blastospore-to-hyphae transition. Branching and hyphal elongation were predominantly observed at this time point. Bars represent 30 µm.

3D1 and 3D7. Branching and hyphal elongation were frequently observed at 48 hai. Surprisingly, high temperature promoted the formation of two new morphologies in the 1A5 strain, with appearances matching pseudohyphae and chlamydospores (asterisks and black arrows, respectively). However, no hyphal growth was observed for this strain. Interestingly, chlamydospore-like cells were found for all strains at 144 hai (black arrows). Cellular differentiation from blastospores to pseudohyphae began in 1A5 at 24 hai, resulting in a series of conjoined elongated cells, characteristic of pseudohyphae[15]. We also observed several swollen cells at 24 hai that we believe represent the initial differentiation from blastospores into chlamydospore-like cells, but the complete differentiation occurred between 48 and 96 hai. Chlamydospore-like cells were observed attached to the ends of pseudohyphae or distal parts of filamentous hyphae, but we also observed chlamydospore-like cells detached from suspensor cells. Chlamydospore-like cells formed in different sizes for all the tested strains. Blastospores incubated in YSB at 18 °C continued to replicate only as blastospores via blastosporulation and were used as controls.

A nutrient-limited environment promotes filamentous growth. We used two defined media to determine the effect of nutritional limitation on cell morphology. Carbon- or nitrogen-depleted medium promoted hyphal growth in all four strains (Fig. 3). In a C-depleted environment (Minimal medium (MM) without

sucrose), cellular differentiation occurred after 24 hours of incubation, when hyphal formation was observed with the first germ tube formed terminally (1A5 and 3D1) or laterally (1E4 and 3D7) (black triangles). Hyphal elongation and branching continued at 48 and 72 hai (data not shown). By 144 hai mycelial growth was predominant, with frequent anastomosis events among hyphae (asterisks). In MM with sucrose, all strains grew as a mixture of blastospores and hyphae, with blastospores budding from filamentous hyphae, showing that the morphological transition is bidirectional (Fig. S1). Blastospores incubated in YSB continued to replicate only as blastospores via blastosporulation (white triangles).

In N-depleted medium (MM without ammonium nitrate), three strains (1A5, 3D1, and 3D7) initially formed hyphae from one apical end, generating the first and second hyphal elongations within 72 hai (Fig. 3). 1E4 responded most quickly to a low-nitrogen environment, with hyphae forming at 48 hai (black triangle) and a network of filamentous hyphae formed at 72 hai. In regular MM all strains grew as a mixture of morphotypes (Fig. S1). Interestingly, the hyphae induced under both carbon and nitrogen limitation were thinner than those produced by high temperature (Fig. 2).

Oxidative stress induces morphological changes in some strains. To determine the effect of oxidative stress on the *Z. tritici* morphology, we examined the growth in presence of hydrogen peroxide (H_2O_2) at two blastospore concentrations. At a high initial cell density (10^5 blastospores/mL), H_2O_2 stimulated hyphal growth in 1E4 up to a concentration of 5 mM (Fig. S2). 1A5, 3D1, and 3D7 continued to replicate as blastospores, but there was a substantial reduction in blastospore formation starting at 5 mM H_2O_2 (Fig. S2). To test whether a lower cell concentration would change the sensitivity of blastospores to oxidative stress, we inoculated flasks with 10^3 blastospores/mL. After 72 hours of incubation in 0.5 mM H_2O_2, strains 1E4 and 3D1 showed apical and lateral hyphal branching (Fig. 4, black triangles), but both strains continued to form blastospores (white triangles). At 1 mM, blastospores from 1E4, 3D1, and 3D7 developed into a mixture of pseudohyphae and regular hyphae (white asterisks and black triangles, respectively). The higher sensitivity at low cell densities suggests that the exogenous H_2O_2 was more rapidly degraded by secreted hydroperoxidase proteins (catalases, peroxidases and catalase-peroxidase) when cell densities were 100X higher. The 1A5 strain did not switch to a different morphotype at any H_2O_2 concentration, continuing to replicate as blastospores. Starting at 2 mM H_2O_2, none of the strains changed their morphology, and blastosporulation ceased, suggesting a cytotoxic effect of H_2O_2 at these concentrations.

Inoculum size effect suggests that quorum sensing may affect the morphological transition. To evaluate the effect of the inoculum size on the morphological transition, we incubated all four strains at five cell densities in two growth conditions shown to induce hyphal growth. After 144 hours of incubation in C-depleted medium at 18 °C, we observed that morphology was independent of cell density for all four strains up to a concentration of 10^5 blastospores/mL (Fig. S3), with most of the blastospores switching to hyphal growth and forming mycelial colonies. However, when the initial cell density was $\geq 10^6$ blastospores/mL, we observed a substantial reduction in the blastospore-to-hyphae transition and in hyphal length. No hyphae formed for 3D1 and 3D7 at initial cell densities of 10^7 blastospores/mL, and they were clearly reduced for 1E4 and 1A5 (Fig. S3).

In YSB at 27 °C we also found that initial inoculum size affected cell morphology (Fig. S3), though there were more pronounced differences among strains in this environment. At 144 hai, starting from the lowest initial cell density (10^3 blastospores/mL), we observed pseudohyphae formation in 1A5, 1E4, and 3D1, and a mixture of pseudohyphae and chlamydospore-like cells in 3D7. At an initial density of 10^4 blastospores/mL, the same phenotypes were found, except that 3D1 formed apical and lateral hyphae. Intermediate initial cell densities (10^5 and 10^6 blastospores/mL) promoted hyphal growth for 1E4, 3D1 and 3D7, but the 3D7 strain grew as a mixture of mycelium and chlamydospore-like cells at 10^6 blastospores/mL. The increase of the inoculum size to 10^7 blastospores/mL induced formation of chlamydospore-like structures in 1E4 and 3D1, and a transition from blastospores to pseudohyphae and chlamydospore-like cells in 3D7. 1A5 was not able to switch to hyphae under high temperatures in any of the initial cell densities and showed chlamydospore-like cell formation from 10^4 blastospores/mL (Fig. S3). The overall pattern of cell density dependence shown here suggests that a quorum-sensing molecule may be controlling the morphological transition, as has been reported for other pleomorphic fungi[41–43].

Chlamydospore-like cells are produced by *Z. tritici*. As far as we know, structures with the same morphology as chlamydospores have not been reported in *Z. tritici*. We aimed to determine whether these chlamydospore-like cells had properties associated with chlamydospores in other fungi. Chlamydospores are survival structures that have thicker cell walls and a high content of lipid droplets[44]. We stained the different morphological cell types of 1A5 with the chitin-binding dye Calcofluor White (CFW) and the lipid droplets dye Nile Red (NR) to measure these properties. The intensity of CFW fluorescence was higher in chlamydospore-like cells (Fig. 5 – free, terminal, and intercalary) compared with blastospores, hyphae, and pseudohyphae that exhibited a weaker fluorescence for CFW. NR staining revealed that chlamydospore-like cells had a high content of lipid droplets, which was also observed for blastospores and pseudohyphae. On the contrary, hyphae showed a lower lipid droplet content than spores, with the exception of the hyphal branching zones as has been reported for other fungi[45]. We then examined the thickness of the cell walls for three cell types using transmission electron microcopy (TEM). TEM showed that the chlamydospore-like cells had thicker cell walls than blastospores and pycnidiospores (Fig. 6). We also found that pseudohyphae and the elongated suspensor cells, where chlamydospores are usually attached to the surrounding mycelium, have a cell wall thickness similar to pycnidiospores. The same pattern of thicker cell walls in chlamydospore-like cells was found for the 3D7 strain (data not shown). On average, chlamydospore-like cells produced by *Z. tritici* had a cell wall thickness of ~460 nm, about four times thicker than the cell walls found in blastospores and pycnidiospores (Fig. 6 - graphics). Despite the thickness of the cell wall, we could not differentiate an extra cell wall layer as reported in chlamydospores from other fungal species[46,47].

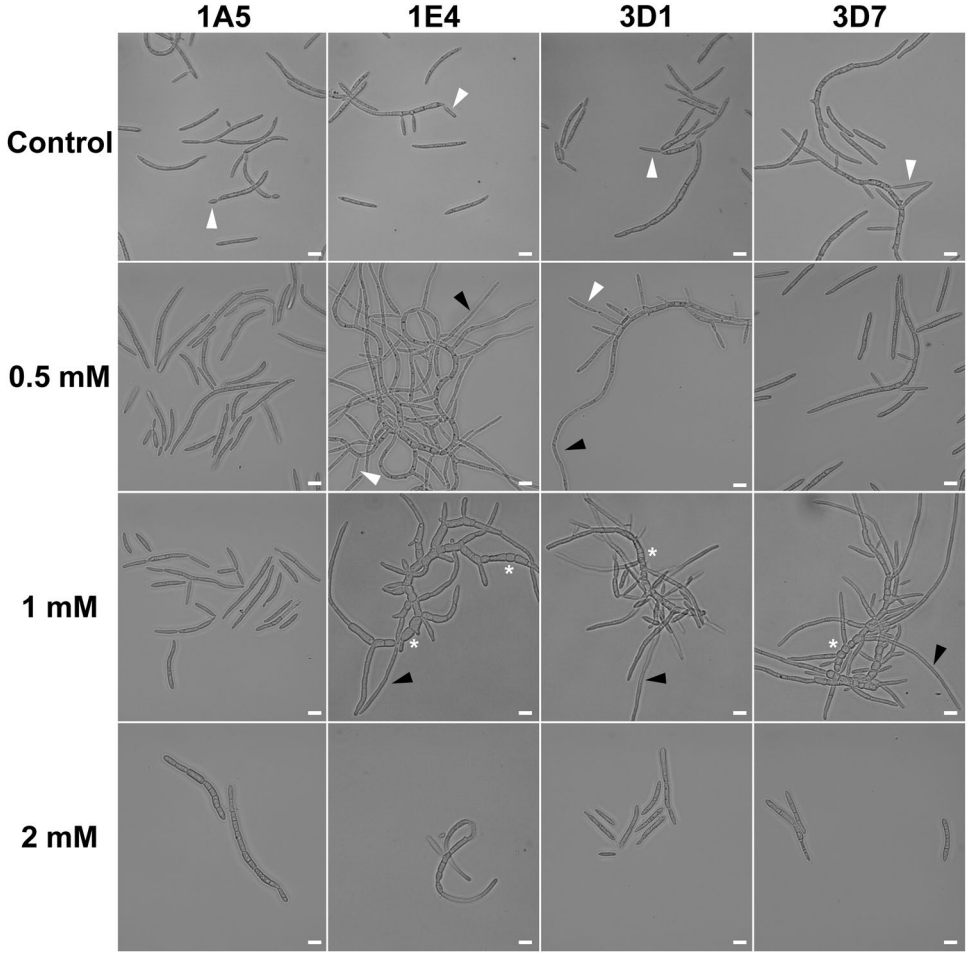

Figure 4. Effect of exogenous oxidative stress induced by H_2O_2 on the cell morphology of four *Zymoseptoria tritici* strains using a low blastospore inoculum density (10^3 blastospore/mL). A nutrient-rich medium (YSB) containing different concentrations of H_2O_2 was used to incubate the strains under oxidative stress for 72 hours. Blastopores kept on YSB medium without addition of H_2O_2 continued to multiply as budding blastospores (white triangles) via blastosporulation and were used as a control. At 0.5 mM, only the 1E4 and 3D1 strains showed hyphal branching and the initial formation of mycelium (black triangles), but both strains continued to form blastospores (white triangles). At 1 mM, blastospores from 1E4, 3D1, and 3D7 grew as a mixture of pseudohyphae (white asterisks) and filamentous hyphae. At 2 mM, none of the strains changed their morphology nor were they able to asexually reproduce via blastosporulation. Blastospores of the 1A5 strain did not switch to different morphotypes in any of the tested concentrations of H_2O_2. Bars represent 10 μm.

To determine if the chlamydospore-like cells are also produced during plant infection, wheat plants were inoculated with pycnidiospores of all four strains expressing cytoplasmic GFP and kept in a greenhouse chamber until pycnidia formation. Microscopic examination of the spore solution harvested from 20-day-old infected leaves showed chlamydospore-like cells mixed among the pycnidiospores (Fig. S4).

The chlamydospore-like cells are metabolically active and highly stress tolerant. The chlamydospore-like cells of 1A5 germinated and produced hyphae. After 12 hours of incubation on water agar (WA) plates, we observed germ tubes emerging from the chlamydospore-like cells, which led to the development of hyphae at 24 hai (Fig. 7, left panel). Blastospores used as controls initially germinated from one apical side, generating the first and second germ tubes within 12 hai. We inoculated wheat with chlamydospore-like cells from GFP-tagged 1A5 to observe by confocal microscopy whether these cells could germinate on the leaf surface. At 24 hpi, free chlamydospore-like cells and chlamydospore-like cells still attached to a suspensor cell produced germ tubes and hyphae on the surface of wheat leaves (Fig. 7, right panel). These results suggest that chlamydospore-like cells may be able to cause infections.

We also investigated whether chlamydospore-like cells share other characteristics of fungal resting spores, such as an ability to resist drought and temperature extremes. Incubation for one day under drought stress reduced viability of blastospores and pseudohyphae by 70%, while the chlamydospore-like cells had a reduction in cell viability of only 23% (Fig. 8A). These rates changed little after 3 days of drought stress. After 5 days of drought stress, the survival rates were 10%, 19%, and 49% for blastospores, pseudohyphae and chlamydospore-like cells,

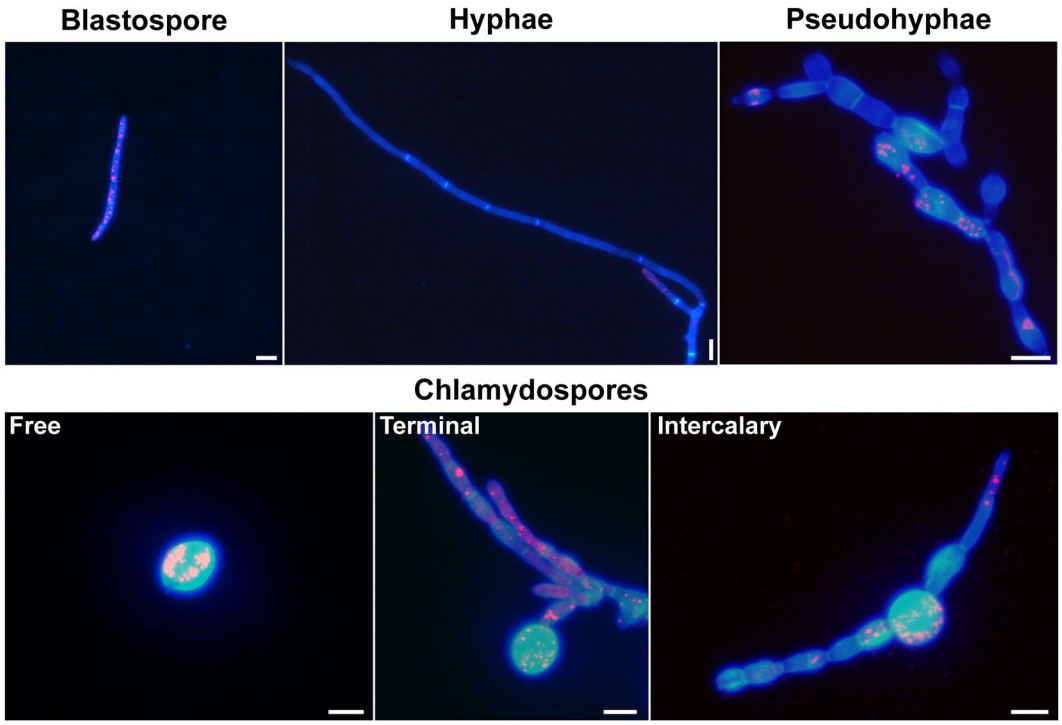

Figure 5. Staining of cell wall chitin and lipid content in the different morphotypes of *Zymoseptoria tritici*. Cell walls were stained with the chitin-binding dye Calcofluor White (blue color) and the lipid droplets were stained with Nile Red (red color). Blastospores, hyphae, and pseudohyphae showed a weaker fluorescence for Calcofluor White compared to free chlamydospores and those formed terminally or intercalarily via suspensor cells. A high accumulation of lipid droplets was observed in chlamydospores, as well as in blastospores and pseudohyphae. Hyphae only showed a high accumulation of lipid droplets in the hyphal branching zone. Bars represent 10 μm.

respectively. After 10 days of drought stress, the chlamydospore-like cells exhibited a survival rate of 50%, significantly higher than the other cell types. In the cold stress experiment, only the chlamydospore-like cells survived the cold shock, with survival rates of 23%, 17%, and 19% after 1 min, 2 min and 3 min in liquid nitrogen, respectively (Fig. 8B). The survival rates of chlamydospore-like cells in liquid nitrogen were not significantly different for the three exposure times. In the heat stress experiment, incubation at 30 °C for 24 hours affected blastospores and chlamydospore-like cells equally, but the 35 °C treatment killed all the blastospores while chlamydospore-like cells and pseudohyphae survived at rates of 12% and 6%, respectively (Fig. 8C). None of the morphotypes survived at 40 °C (Fig. 8C). For all tested environmental stresses, chlamydospore-like cells were the morphotype that exhibited the highest survival rate, suggesting that this structure exhibits ecological characteristics typical for fungal resting spores that enable improved survival to different stresses encountered in nature.

Mycelial growth is co-regulated with the expression of virulence-related genes. Aiming to identify genes associated with mycelial growth in nutrient-poor environments, we compared the transcriptomes from blastospores and two different hyphal-inducing conditions, C-depleted medium and early wheat infection (7 days post infection - dpi), among the four strains (Fig. S5) (data set in NCBI SRA SRP152081). The total number of sequencing reads and mapped reads per strain under different growth conditions is given in Table S1. Pairwise comparisons were used to identify the differentially expressed genes between strains and conditions. The proportion of strain-specific upregulated genes during blastospore growth ranged from 5.5% of the genome (659 genes, 1E4 strain) to 7.9% (951 genes, 1A5 strain) when compared to C-depleted medium, and from 6.5% of the genome (785 genes, 1A5 strain) to 10.6% (1271 genes, 3D1 strain) when compared to wheat infection (Fig. S6; Tables S2 and S3). On the other hand, the proportion of strain-specific upregulated genes during mycelial growth ranged from 10.6% of the genome (1241 genes, 3D7 strain) to 12.4% (1500 genes, 1A5 strain) in C-depleted medium, and from 4.7% of the genome (567 genes, 3D1 strain) to 8.7% (1023 genes, 3D7 strain) in wheat infection, when both conditions are compared to YSB (Fig. S7; Tables S4 and S5). A total of 4888, 5296, 5323, and 6003 genes were differentially expressed between blastospore and hyphal growth in 1A5, 1E4, 3D1, and 3D7, respectively.

The upregulated genes shared among all four strains for each morphology were selected for further analysis. Two distinct sets of 134 genes shared among the four strains were identified in both comparisons. The first set named "blastospore growth" is composed of genes that were upregulated during the blastospore growth phase: these genes were upregulated in YSB compared to C-depleted medium and 7 dpi wheat infection, FDR $\leq$ 0.01 (Fig. S8A; Table S6). The second set named "mycelial growth" consists of genes that were upregulated during the mycelial growth phase: these genes were upregulated both in C-depleted medium and 7 dpi wheat infection

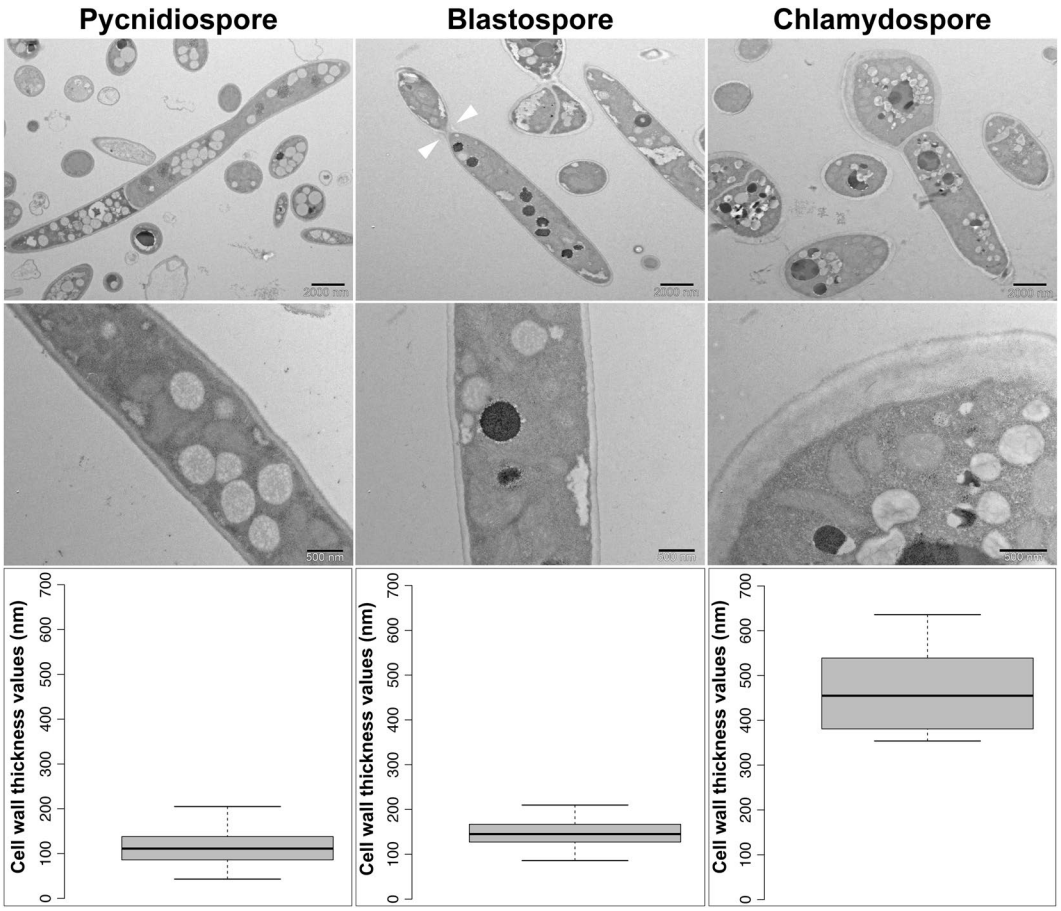

Figure 6. Chlamydospore cells produced by *Zymoseptoria tritici* have thicker cell walls than pycnidiospores and blastospores. Images obtained by transmission electron microscopy were used to measure the cell wall thickness of different morphotypes from the 1A5 strain. White triangles point to a detaching daughter cell budding from a blastospore mother cell. Twenty micrographs of each morphotype were randomly selected to measure the cell wall thickness. Comparisons of cell wall thickness showed that chlamydospore-like cell walls are four times thicker than the cell walls in blastospores and pycnidiospores. Two different magnifications are shown for each morphotype: top panels scale bar = 2000 nm (low magnification), bottom panels scale bar = 500 nm (high magnification).

compared to YSB, FDR $\leq$ 0.01 (Fig. S8B; Table S7). For both comparisons, the sets of genes that do not overlap represent genes with a strain-specific expression profile for each growth condition (Figs S6 and S7; Tables S2–S5).

Among the 134 shared genes that are significantly upregulated during blastospore growth, 20% are annotated as *hypothetical proteins* (Fig. 9A; Table S6). The remaining 107 genes are divided into fourteen biological process categories, with *metabolism* being the most represented term (44%). This category was composed mainly of non-secreted enzymes, including oxidoreductases (n = 11), dehydrogenases (n = 8), hydrolases (n = 7), and transferases (n = 9) (Fig. 9A). No enrichment was found for any other category. However, seven genes from other categories were already described in other fungi to be involved in blastosporulation (Table S8). As expected, genes related to vegetative blastospore growth were highly expressed in nutrient-rich medium - the environment most conducive for this morphotype (Fig. S8C).

Among the 134 genes that were upregulated in all strains during mycelial growth, we observed an enrichment of secreted proteins (32%) associated with fungal virulence, including *candidate effectors* (small secreted proteins - SSPs), *secreted proteases*, *secreted glycosidases*, *secreted chloroperoxidases, cell wall hydrolases, hydrophobins*, and *hydrophobic surface binding proteins* (Fig. 9B; Tables S7 and S9). Overall, these virulence-associated genes were upregulated in C-depleted medium and during all stages of plant infection, albeit with a reduction in expression during the saprophytic phase of infection (at 28 dpi). The peak of expression of these virulence-associated genes preceded the first visual symptoms of infection, at 12 dpi for 1A5 and 3D7, and at 14 dpi for 1E4 and 3D1 (Fig. S8D), as previously reported for some of these gene categories[48]. These patterns suggest that mycelial growth is co-regulated with the expression of genes relevant for virulence even in the absence of the host. We also detected the upregulation of six genes related to cellular morphogenesis (Table S10). The transcription profiles of these genes showed an upregulation in both mycelial growth conditions (C-depleted medium and 7 dpi wheat infection) with the peak of expression occurring at 7 dpi for all four strains (Fig. S8E).

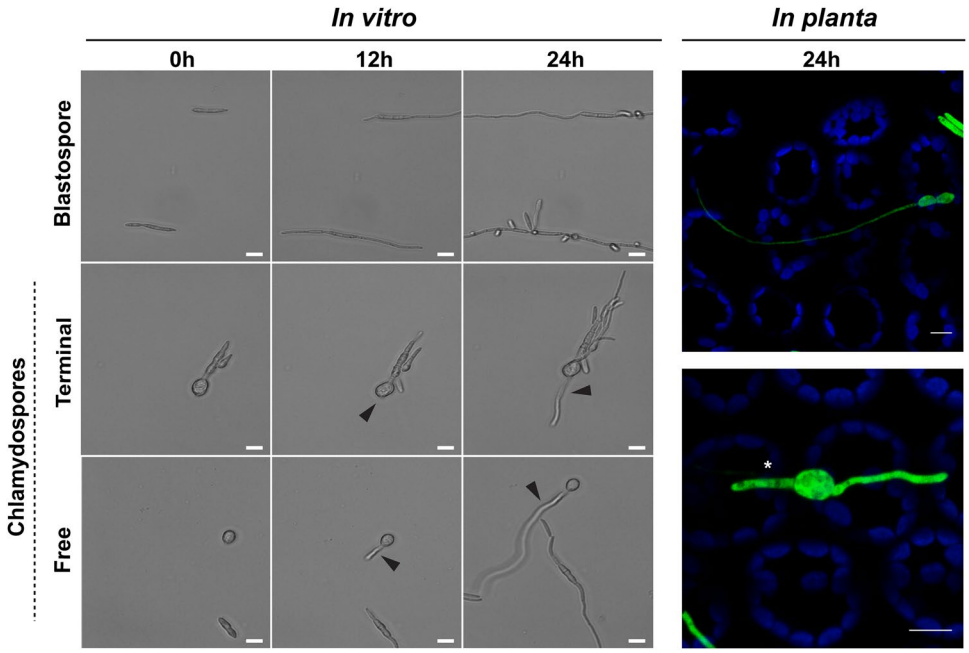

Figure 7. Chlamydospores produced by *Zymoseptoria tritici* are able to germinate both *in vitro* and on the surface of wheat leaves. Blastospores were used as a control for *in vitro* assays. Apical germination and hyphal elongation were observed after 12 hours of incubation on water agar (WA) plates at 18 °C. At 24 hai, blastosporulation was observed from the germinated blastospores. Terminal chlamydospores formed via suspensor cells and free chlamydospores initiated their germination (black triangles) after 12 h of incubation on water agar. Hyphal elongation was obvious at 24 h. Bars represent 10 μm. On the surface of wheat leaves (right panel), free chlamydospores (upper image) and terminal chlamydospores (lower image) from a GFP-tagged 1A5 strain (green color) produced germ tubes after 24 hours of infection. Blue color corresponds to the autofluorescence detected from chlorophyll A. Asterisk indicates the suspensor cells where chlamydospores are attached. Bars represent 8 μm.

Discussion

Fungi evolved to perceive a wide array of environmental signals and reprogram their cellular responses accordingly to maximize their fitness. Though much research has been oriented around morphological changes and their associated transcriptional pathways in response to different stressors in fungal pathogens of humans[10,18,49], knowledge in this area is limited for plant pathogens. Our study shows how different environmental stresses can affect cellular morphologies in the wheat pathogen *Z. tritici*. We also demonstrate the phenotypic plasticity of this fungus in response to environmental changes, as well as differential responses to the same environments among strains. An unexpected outcome of this study was the discovery of two novel morphotypes, one of which may have important epidemiological consequences.

Another finding with epidemiological implications was to demonstrate that blastospores can form from germinating pycnidiospores on the surface of wheat leaves. This possibility was proposed more than 30 years ago[50,51], but was not followed up in subsequent studies. The formation of blastospores during *in vitro* growth in nutrient-rich medium is why *Z. tritici* has long been considered to be a dimorphic fungus and also gave rise to the "*zymo*" part of the genus name[52], but until now it was not clear if the blastospores could also form on leaf surfaces in nature. Our experiments confirmed that blastospores are produced during a natural infection. It remains unclear whether blastospores make a significant contribution to the development of epidemics. Given their small size and increasing abundance over time, we hypothesize that they may play an important role in the explosive increase in STB that can occur following prolonged rainy periods that last for several days[50,53].

We found that several environmental stresses can affect morphological transitions in strain-specific ways for four natural *Z. tritici* strains sampled from the same Swiss population. All four strains switched to hyphal growth in a nutrient-poor minimal medium. Morphological changes induced by limited nutrients have also been described in other dimorphic plant pathogenic fungi distributed across different phyla[9,54]. Nutrients are present on the leaf surface in very small quantities and are usually surrounded by epicuticular waxes[55]. As a result, plant pathogens typically experience nutritient limitations while growing on leaves. It is thought that secreted enzymes, including plant cell wall degrading enzymes (PCWDEs) such as cutinases, are required to obtain nutrients during this stage of development, but *Z. tritici* has few PCWDEs compared to other fungi[56], suggesting that the perception of a nutrient-limited environment may act as a stimulus to induce a switch to an exploratory morphotype (hyphae) that can better explore the environment for food. We found a significant increase in the frequency of anastomosis events during mycelium formation under nutrient-limited conditions. Mycelial networks formed by anastomosis enable a shared cytoplasmic flow that can more efficiently distribute water, nutrients, and signals within a fungal colony[57,58]. Moreover, hyphal fusions were shown to be required for virulence for some plant

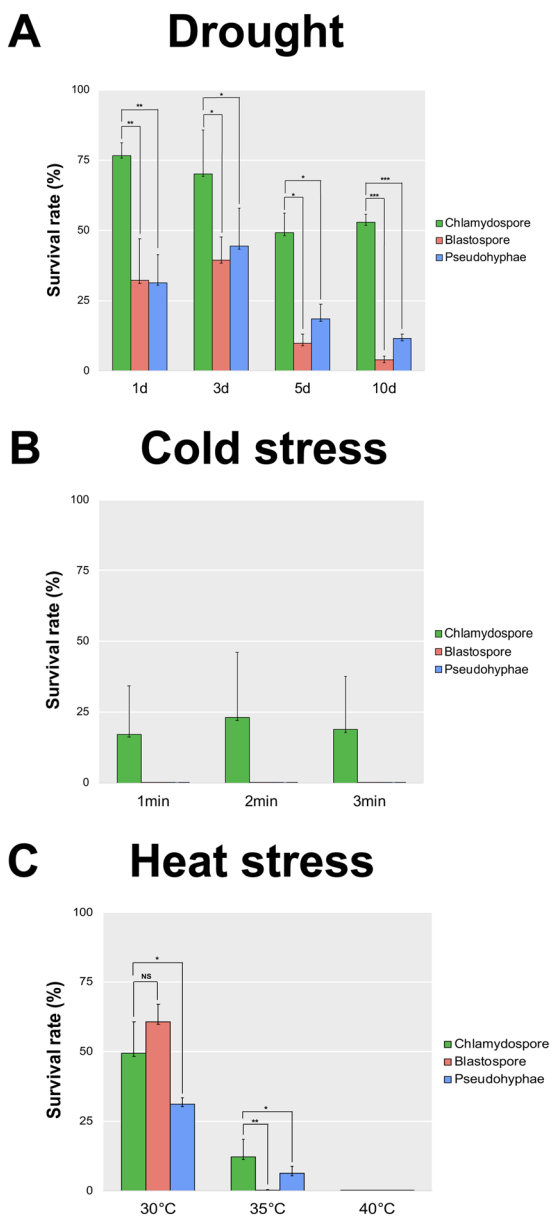

Figure 8. Chlamydospores produced by *Zymoseptoria tritici* are more tolerant to stress than blastospores and pseudohyphae. Survival rate (%) was estimated based upon the number of colonies formed after exposure to the stressful environment compared to the number of colonies formed in the control environment after seven days. All stress assays were performed using different morphotypes from the 1A5 strain. (**A**) Blastospores, pseudohyphae and chlamydospore cells were kept for 1, 3, 5, and 10 days in a sealed box containing anhydrous silica gel to produce a dry environment. This simulated drought stress affected blastospore and pseudohyphae survival over time. Chlamydospores were less affected and exhibited a survival rate of 50% after 10 days under drought stress. (**B**) The same three morphotypes were subjected to a cold shock. Blastospores, pseudohyphae, and chlamydospores were submerged in liquid nitrogen for 1, 2, and 3 minutes at −196 °C. Only chlamydospores survived this cold stress. (**C**) The same three morphotypes were subjected to heat stress based on incubation for 24 hours at 30 °C, 35 °C or 40 °C. Blastospores and chlamydospores were equally affected at 30 °C. The incubation at 35 °C killed all the blastospores, while chlamydospore survived at a 12% rate, double the rate observed for pseudohyphae (6%). No colonies were observed after incubation at 40 °C. One star indicates that the adjusted p value is <0.05, two stars indicates that the p value is <0.005, and three stars indicates that the p value is <0.0005. NS indicates no significant difference.

pathogens[59,60]. We hypothesize that hyphal anastomosis provides benefits during epiphytic growth of germinating *Z. tritici* pycnidiospores prior to stomatal penetration, with anastomosis facilitating colony establishment and increasing strain fitness during colonization of the host.

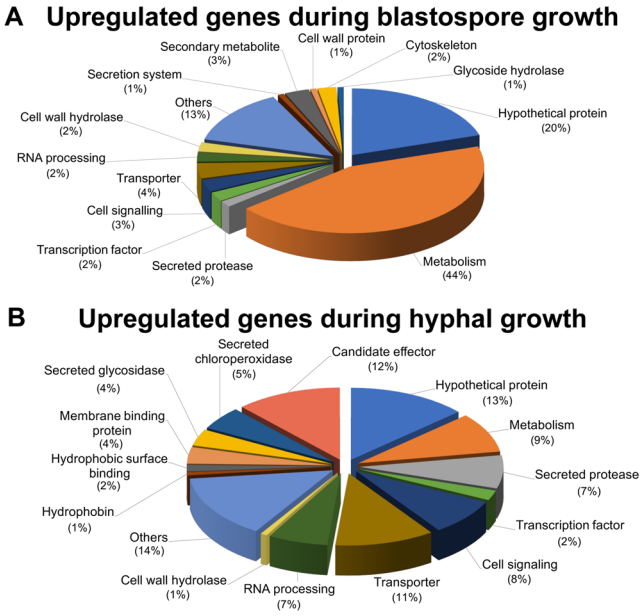

Figure 9. Transcriptome signatures of blastospore and mycelial growth phases organized based on enrichment of molecular functional terms. (**A**) Common upregulated genes during the blastospore growth phase among the *Zymoseptoria tritici* strains. (**B**) Common upregulated genes for the mycelial growth phase among the *Z. tritici* strains.

The oxidative burst is a ubiquitous plant defense response to pathogen infection, resulting in a rapid release of reactive oxygen species (ROS), including hydrogen peroxide (H_2O_2)[61]. The ROS produced during plant defense were proposed to have various functions, including activation of plant defense-related genes and a direct antimicrobial effect that inhibits pathogen growth[62–64]. Though many studies have demonstrated its antimicrobial effects, the effects of H_2O_2 on morphological transitions remain largely unexplored. In *Candida albicans*, H_2O_2 induces hyphal differentiation in a dose-dependent manner[65]. Our results show that blastospores of three out of four *Z. tritici* strains switch to hyphae and pseudohyphae when exposed to H_2O_2 in a dose-dependent manner. A cell density dependence was also found. The different cell density responses suggest that the H_2O_2 is more rapidly metabolized by fungal hydroperoxidase proteins (catalases, peroxidases and catalase-peroxidase), leading to lower toxicity at higher cell densities. Several genes encoding peroxidases and catalase-peroxidases were identified in the genome of *Z. tritici*[66,67], which may explain the observed phenotype. The inability of 1A5 to differentiate hyphae from blastospores at any H_2O_2 concentration suggests that this strain either cannot sense oxidative stress or that it possesses a more efficient antioxidant response that can neutralize the effects of H_2O_2. Further experiments will be needed to test these hypotheses.

Temperature is an important abiotic factor that strongly affects growth, reproduction, and development in fungi[68,69]. Thermally dimorphic human fungal pathogens usually undergo morphological transitions in response to host temperature[54,70]. *Z. tritici* is the first plant pathogen shown to undergo morphological transitions after exposure to high temperatures[31,68]. Our experiments showed that a change in temperature from 18 °C to 27 °C triggered hyphal growth in three out of four tested *Z. tritici* strains. For these three strains, an increase in hyphal elongation and formation of branches occurred soon after exposure to the higher temperature. The hyphae formed at a high temperature appeared thicker than those formed under nutrient limitations and it is not clear whether they could infect host tissues.

An unexpected outcome of this study was the discovery of chlamydospore-like cells in *Z. tritici*. The preponderance of evidence indicates that these cells are truly chlamydospores. Their morphology matched the chlamydospores described in other fungi: spherical, thick-walled cells with a high lipid content that form either intercalated or at the ends of filamentous hyphae and occasionally on pseudohyphae[20,71]. We also showed that these cells were able to survive and germinate following several stresses that killed other cell types, including desiccation and high and low temperatures, consistent with the function of chlamydospores as long-term survival structures in other fungi[19–21,72]. We conclude that *Z. tritici* produces chlamydospores.

As far as we know, this is the first time that chlamydospores have been found in a plant pathogen that is thought to mainly inhabit the phyllosphere. Though chlamydospores were especially prominent in the 1A5 strain at high temperature, we observed chlamydospore production in all four strains both *in vitro* and *in planta*. We hypothesize that the chlamydospores produced by *Z. tritici* may contribute an important source of inoculum that can survive between growing seasons and perhaps form a long-term spore-bank that can persist for many years in wheat-growing regions. Chlamydospores may also contribute to long-distance movement of the pathogen on infested straw or seeds. These properties could impact the management of septoria tritici blotch (STB), but additional studies will be needed to understand the roles played by chlamydospores during the STB disease cycle.

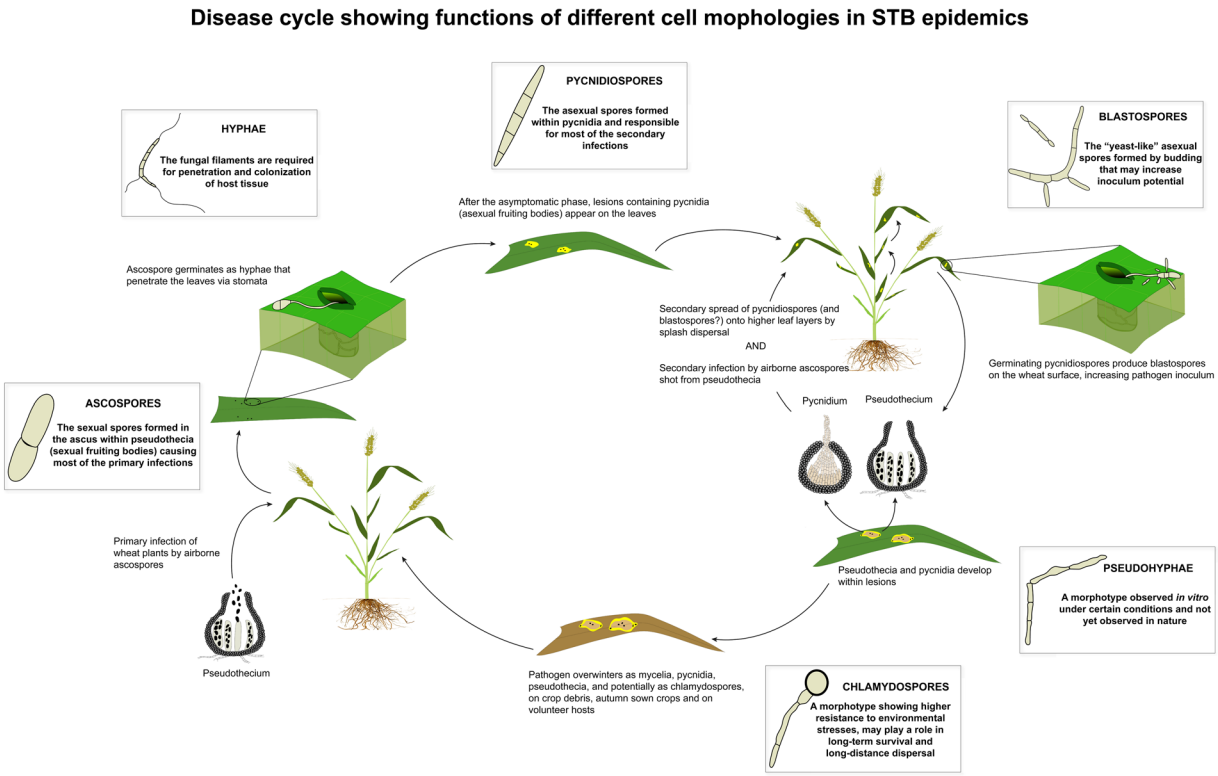

Figure 10. Illustration showing the disease cycle of septoria tritici blotch, including the known cell morphologies and their associated biological functions for the causal agent *Zymoseptoria tritici*.

The transcriptome sequencing identified genes associated with mycelial growth in *Z. tritici*. Starvation induces the expression of virulence-related genes in other plant pathogenic fungi[73,74]. In *Z. tritici*, we found that genes potentially relevant for virulence, including secreted hydrolytic proteins and candidate effectors, were upregulated in both hyphae-inducing conditions (carbon-depleted medium and *in planta*), suggesting that genes controlling morphogenesis and virulence may be co-regulated under nutrient-limited conditions. In *C. albicans*, genes related to hyphal growth are co-regulated by transcription factors that affect expression of genes involved in virulence[5,7]. However, it is important to note that not every virulence function is connected to morphogenesis. The specific genes involved in the activation and regulation of these morphological transitions remain unknown for *Z. tritici*.

In conclusion, we demonstrate that a fungal plant pathogen responds morphologically to diverse environmental stresses, and we propose distinct biological roles for different morphotypes (Fig. 10). We also illustrate the advantage of including different natural strains when studying the response of a species to environmental stresses, as we found different morphological responses among the tested strains. Our findings provide important new insights into the *Z. tritici*-wheat pathosystem including: (1) the formation of blastospores from germinating pycnidiospores on the surface of wheat leaves, enabling a potentially significant increase in inoculum size; (2) the phenotypic plasticity of *Z. tritici* in response to different environmental changes; (3) the ability to produce distinct morphotypes; (4) the discovery of chlamydospores that may help the fungus to survive stressful conditions; (5) the co-regulation of morphogenesis and virulence. These findings position *Z. tritici* as an excellent model organism to explore how morphological changes can affect adaptation to different environments in fungal plant pathogens.

Materials and Methods

Fungal strains, environmental stimuli, and growth conditions. Four previously characterized *Zymoseptoria tritici* strains (ST99CH_1A5, ST99CH_1E4, ST99CH_3D1, and ST99CH_3D7, abbreviated as 1A5, 1E4, 3D1, and 3D7, respectively)[75,76], sampled from two naturally infected wheat fields separated by 10 km in 1999 and differing for many quantitative traits, including thermal adaptation and virulence[48,75,77,78], were used in this study. Strains expressing cytoplasmic GFP[79] were provided by Andrea Sanchez-Vallet after being generated by Sreedhar Kilaru and Gero Steinberg as described in Zala *et al.*[80]. All strains were grown in YSB (yeast extract 10 g/L and sucrose 10 g/L; pH 6.8). Depending on the tested environment, we used either YSB or a defined salts medium (Minimal Medium – MM, pH 5.8)[81]. Each strain was stored in glycerol at −80 °C until required and then recovered in YSB medium incubated at 18 °C for three days. For nutrient limitation experiments, the cells were washed three times with sterile distilled water to remove any remaining nutrients prior to placing them into nutrient-limited conditions. Cell concentrations were determined by counting blastospores using a KOVA cell chamber system (KOVA International Inc., USA).

Plant infection assay to assess blastospore production from pycnidiospores. The susceptible wheat cultivar Drifter was used in all experiments. Plant growth conditions were described earlier[82]. All infection assays used 16-day-old plants. A blastospore suspension of the 3D7 strain tagged with cytoplasmic GFP produced after 3 days of growth in YSB at 18 °C was filtered through two layers of cheesecloth and diluted to a final concentration of 10^6 blastospores/mL in 30 mL of sterile water supplemented with 0.1% (v/v) Tween 20. Spore suspensions were applied to run-off using a sprayer and the plants were kept for three days in sealed plastic bags, followed by 21 days in a greenhouse. Leaves with pycnidia were harvested and transferred to a 50 ml Falcon tube containing sterile water and gently agitated to harvest the pycnidiospores. GFP-tagged 3D7 pycnidiospore suspensions were adjusted to a final concentration of 10^6 pycnidiospores/mL and a new batch of plants was inoculated as described above. The inoculated plants were kept in plastic bags at 100% humidity until they were examined for blastospores at 24 and 48 hai.

Effect of temperature on growth morphology. Blastospores of each strain were inoculated on YSB at a final concentration of 10^5 blastospores/mL. Three flasks were incubated at 18 °C (as control) and three at 27 °C for four days. An aliquot was taken from each flask at 8, 24, 48, 96, and 144 hai to monitor cell morphology by light microscopy using a Leica DM2500 microscope with LAS version 4.6.0 software. These experiments were repeated three times.

Effect of nutrient limitation on growth morphology. MM was used to monitor the transition in growth morphologies under different nutrient limitations. The effect of carbon depletion was assessed by adding each strain at a final concentration of 10^5 blastospores/mL into either regular MM, which contains sucrose as the main carbon source, or into MM without sucrose (C-depleted medium) and incubated at 18 °C. The cell morphology was observed by light microscopy every 24 hours until 144 hai. The effect of nitrogen depletion was determined using MM lacking ammonium nitrate (N-depleted medium), which is normally present in MM as the main nitrogen source. We compared the growth morphologies of cells growing in MM with and without ammonium nitrate by light microscopy during 96 hours of incubation at 18 °C. The growth morphologies in both nutrient-limited conditions were compared to the morphologies found in the nutrient-rich YSB. Experiments were repeated three times for each nutrient environment.

Effect of oxidative stress on growth morphology. H_2O_2 was added into YSB at different concentrations (0, 0.5, 1, 2, 5, and 10 mM) to induce different levels of exogenous oxidative stress. Each strain was added to a final concentration of 10^5 blastospores/mL and incubated at 18 °C. Morphological changes and cellular morphologies were observed by light microscopy at 72 hai. To determine whether a lower concentration of blastospores promotes a higher susceptibility to oxidative stress, we performed the same experiment using a final concentration of 10^3 blastospores/mL. These experiments were repeated twice.

Effect of inoculum size on growth morphology. Flasks containing YSB or C-depleted medium were inoculated with a final cell density of 10^7 blastospores/mL, followed by a 10X serial dilution to a concentration of 10^3 blastospores/mL. Flasks containing C-depleted medium were incubated at 18 °C and flasks with YSB were incubated at 27 °C. Cell morphology was determined every 24 hours using light microscopy over 144 hours of incubation. These experiments were repeated three times.

Fluorescence microscopy to quantify chitin and lipids in different morphotypes. Blastospores of 1A5 were inoculated into YSB to a final concentration of 10^5 blastospores/mL and incubated at 18 °C or 27 °C to induce blastosporulation or chlamydospore-like formation, respectively. 1A5 was also inoculated at the same concentration into C-depleted medium and incubated at 18 °C to induce hyphal growth. After four days of incubation, the resulting cells were harvested and fixed with 70% (v/v) ethanol for 30 minutes, followed by three washes with phosphate-buffered saline (PBS). The cells were stained with 1 μg/mL of CFW and 2.5 μg/mL of NR (both reagents from Sigma-Aldrich Chemie Gmbh, Munich, Germany) for 15 minutes. The stained cells were viewed with a Leica DM2500 fluorescence microscope with LAS version 4.6.0 software, using a UV filter system for CFW consisting of a BP excitation filter at 340–380 nm and a long pass emission filter (>425 nm), and a red filter system for NR consisting of a BP excitation filter at 546/10 nm and an emission filter at 585/40 nm.

Transmission electron microscopy. Cells of 1A5 and 3D7 were collected after 4 days of growth in YSB at 18 °C or 27 °C, from blastospore- or chlamydospore-bearing solutions, respectively. Pycnidiospores for each strain were harvested from infected wheat plants. Samples were prepared using microwave-assisted fixation in 0.1 M cacodylate buffer (2.5% glutaraldehyde and 2% paraformaldehyde), using a PELCO Biowave (Ted Pella, California, USA), followed by embedding in 2% low melting temperature agarose (SeaPlaque Agarose, FMC Corporation, USA). A second step of microwave-assisted fixation was used after embedding in agarose. Before resin infiltration, the samples went through two steps of post-fixation, first in osmium tetroxide (OsO4) in 0.1 M cacodylate buffer and then in 1% uranyl acetate (UrAc), followed by a graded series of ethanol washes for dehydration (25%, 50%, 75%, 90%, and 100%). Samples were infiltrated with Spurr resin and polymerized at 60 °C for 48 hours. Ultrathin sections (60 nm) were cut using the Leica Ultracut FC6 (Leica Microsystem, Vienna) and then transferred to formvar coated carbon grids, followed by post-staining with uranyl acetate and lead citrate. Micrographs were collected using a Morgagni 268 transmission electron microscope operating at 100 kV and using a CCD (1376 × 1032 pixel) camera. Twenty micrographs of each morphotype were randomly selected to measure the cell wall thickness using ImageJ software[83].

Germination of chlamydospore-like cells and their survival under stress. Chlamydospore-like cells and blastospores of the 1A5 strain were harvested from YSB after 4 days of growth at 27 °C or 18 °C,

respectively, and their concentrations were adjusted to ~10^5 cells/mL. 10 μL was spotted onto WA (1% agar in water) and the plates were incubated at 18 °C. Germ tube formation was checked at 0, 12, and 24 hours after inoculation by light microscopy.

To determine whether chlamydospore-like cells differ in their ability to survive environmental stresses compared to blastospores and pseudohyphae, we exposed 8×10^3 cells/mL of each morphotype to different stresses, including drought and extreme temperatures.

For drought stress, 200 μL of each cell solution were spread onto Amersham Hybond™ N^+ nylon membranes (GE Healthcare Life Sciences, Chicago, Illinois) and dried in a sterile Petri dish placed on a sterile bench in a laminar flow hood. The Petri dishes were then placed into a sealed box containing anhydrous silica gel for 1, 3, 5, or 10 days. After the drought stress, the membranes were placed onto YMA plates (4 g/L yeast extract, 4 g/L malt extract, 4 g/L sucrose, and 12 g/L agar), incubated at 18 °C and colony formation was monitored. Control membranes containing each morphotype were transferred directly to YMA plates without any drying treatments.

For cold stress, 300 μL aliquots of each cell solution were submerged into liquid nitrogen for 1, 2, or 3 minutes, and 200 μL of the thawed cell solution were spread onto YMA plates. Control samples were incubated at room temperature. For heat stress, 200 μL aliquots of each morphotype were incubated for 24 hours at 30, 35, or 40 °C, followed by plating on YMA. Controls were kept at 18 °C. YMA plates from control and treated samples were incubated at 18 °C for seven days. The assessment was based on four technical replicates for each morphotype and treatment. Survival rates for each cell type were estimated based on the number of colonies formed after exposure to the stressful conditions compared to the number of colonies formed by the controls. A t-test statistic was used to test the hypothesis that chlamydospores were more stress tolerant than other morphotypes. All survival experiments under stress conditions were repeated three times.

The formation and germination of chlamydospore-like cells on wheat plants. To determine whether chlamydospore-like cells produce germ tubes and initiate hyphal growth after coming into contact with the host, wheat plants were grown as described earlier and then inoculated with chlamydospore-like cells from the 1A5 strain tagged with cytoplasmic GFP. Production of chlamydospore-like cells was induced using high temperature (YSB at 27 °C) as described earlier. The suspension of chlamydospore-like cells was prepared and concentrations were standardized as described for blastospore infections. The inoculation procedure was the same except the inoculated plants were kept in plastic bags for only 24 hours.

To observe formation of chlamydospore-like cells *in planta*, infected leaves from wheat plants inoculated with GFP-tagged pycnidiospores of all tested strains were harvested at 20 dpi. The infected leaves were incubated in a humidity chamber for 24 hours, followed by washes with sterile distilled water to collect the released spores. The resulting spore suspension was checked for chlamydospore-like cells using a fluorescent microcope with a GFP filter consisting of a BP excitation filter at 480/40 nm and a BP emission filter at 527/30 nm.

Confocal microscopy of germinated pycnidiospores and chlamydospore-like cells on wheat leaves. Confocal images were obtained using a Zeiss LSM 780 inverted microscope with ZEN Black 2012 software. An argon laser at 500 nm was used to excite GFP fluorescence and chloroplast autofluorescence with an emission wavelength of 490–535 nm and 624–682 nm, respectively. Wheat plants inoculated with GFP-tagged 3D7 pycnidiospores were checked at 24 and 48 hai to determine whether pycnidiospores produced blastospores on the leaf surface. Plants inoculated with GFP-tagged 1A5 chlamydospore-like cells were checked at 24 hai to observe germination of the chlamydospore-like cells.

RNA extraction, library preparation, and sequencing. Flasks containing a final concentration of 10^5 blastospores/mL in YSB or C-depleted medium were incubated for four days at 18 °C to induce blastosporulation or mycelial growth, respectively. Total RNA was extracted from three replicates per strain and condition by using TRIzol (Thermo Fisher Scientific, Waltham, Massachusetts) following the manufacturer's instructions. RNA concentration and quality were checked using a Qubit fluorometer (Thermo Fisher Scientific, Waltham, Massachusetts) and a TapeStation 2200 (Agilent, Santa Clara, California). Only samples showing good ribosomal RNA bands without RNA degradation and no DNA contamination were used for sequencing. A Truseq stranded mRNA kit (Illumina Inc., San Diego, CA, USA) was used for library preparation, and ribosomal RNA was depleted by polyA enrichment. The quality and quantity of the enriched libraries were assessed using a Qubit fluorometer (Thermo Fisher Scientific) and TapeStation (Agilent). Libraries were sequenced on the Illumina HiSeq 2500 using 2×100 bp paired-end reads.

Transcriptome mapping and quantification. The sequencing adapters and reads shorter than 15 bp were trimmed from raw Illumina reads using Trimmomatic v.0.36[84] with the following settings: ILLUMINACLIP:TrueSeq3-PE.fa:2:30:10, LEADING:2 TRAILING:2, SLIDINGWINDOW:4:15 MINLEN:15. Filtered reads of each *Z. tritici* strain for the most common growth morphologies (blastospores and mycelial growth) were mapped against their respective genomes using Tophat v.2.0.13[85]. HTSeq-count v.0.6.1 was used to calculate the gene counts[86]. Mapped reads with more than one reported alignment were excluded from further analyses. We applied the TMM (trimmed mean of M values) method implemented in the Bioconductor edgeR v.3.12.0 package to normalize the gene counts and to calculate the differentially expressed genes under each condition[87,88] based on pairwise comparisons. Only genes with average counts per million reads per sample >1 for at least one growth condition were counted as expressed genes. The Benjamin-Hochberg false discovery rate (FDR) correction was used to adjust p-values based on the Fisher exact test. Only genes with adjusted p-values of FDR ≤ 0.01 were included in further analyses.

Transcription profile analysis. To identify the specific transcriptome signatures associated with blastospore and mycelial growth forms, we used three distinct datasets: (1) transcriptomes of four *Z. tritici* strains during blastospore growth in YSB medium; (2) transcriptomes of four *Z. tritici* strains during mycelial growth in

C-depleted medium, and (3) published transcriptomes of the four tested strains during wheat infection at 7 dpi (datasets in NCBI SRA SRP077418)[48], a condition that also induces hyphal growth (Fig. S5). These genes were analysed using the Venny 2.1 program[89], to identify overlapping genes among all four strains and both growth morphologies (blastospore *vs*. mycelium). Specific transcriptome signatures were identified based on the differentially expressed genes that were shared among all four strains and growth forms, according to the *Z. tritici* reference genome annotations[90,91]. For example, we considered as mycelial growth-related genes only those differentially expressed genes that were shared among all four isolates during growth in C-depleted medium and wheat infection at 7 dpi. To define the blastospore growth-related genes, we considered only the differentially expressed genes among all four isolates during growth in YSB. We also used the published transcriptomes of different stages of wheat infection[48] to interpret the expression profiles of some genes under both axenic and *in planta* conditions. The $\log_2$-transformed CPM values of those genes were plotted using the R package ggplot2[92].

References

1. Brown, A. J. P., Cowen, L. E., di Pietro, A. & Quinn, J. Stress Adaptation. *Microbiol Spectr* **5**, https://doi.org/10.1128/microbiolspec.FUNK-0048-2016 (2017).
2. Lin, X., Alspaugh, J. A., Liu, H. & Harris, S. Fungal morphogenesis. *Cold Spring Harb Perspect Med* **5**, a019679, https://doi.org/10.1101/cshperspect.a019679 (2014).
3. Mayer, F. L., Wilson, D. & Hube, B. Candida albicans pathogenicity mechanisms. *Virulence* **4**, 119–128, https://doi.org/10.4161/viru.22913 (2013).
4. Wang, L. & Lin, X. Morphogenesis in fungal pathogenicity: shape, size, and surface. *PLoS Pathog* **8**, e1003027, https://doi.org/10.1371/journal.ppat.1003027 (2012).
5. Kumamoto, C. A. & Vinces, M. D. Contributions of hyphae and hypha-co-regulated genes to Candida albicans virulence. *Cell Microbiol* **7**, 1546–1554, https://doi.org/10.1111/j.1462-5822.2005.00616.x (2005).
6. Brand, A. Hyphal growth in human fungal pathogens and its role in virulence. *International Journal of Microbiology* **2012**, 1–11, https://doi.org/10.1155/2012/517529 (2012).
7. Thompson, D. S., Carlisle, P. L. & Kadosh, D. Coevolution of morphology and virulence in Candida species. *Eukaryot Cell* **10**, 1173–1182, https://doi.org/10.1128/EC.05085-11 (2011).
8. Lübbehüsen, T. L., Nielsen, J. & McIntyre, M. Morphology and physiology of the dimorphic fungus Mucor circinelloides (syn. M. racemosus) during anaerobic growth. *Mycological Research* **107**, 223–230, https://doi.org/10.1017/s0953756203007299 (2003).
9. Nadal, M., Garcia-Pedrajas, M. D. & Gold, S. E. Dimorphism in fungal plant pathogens. *FEMS Microbiol Lett* **284**, 127–134, https://doi.org/10.1111/j.1574-6968.2008.01173.x (2008).
10. Klein, B. S. & Tebbets, B. Dimorphism and virulence in fungi. *Curr Opin Microbiol* **10**, 314–319, https://doi.org/10.1016/j.mib.2007.04.002 (2007).
11. Nigg, M., Laroche, J., Landry, C. R. & Bernier, L. RNAseq analysis highlights specific transcriptome signatures of yeast and mycelial growth phases in the Dutch Elm Disease fungus Ophiostoma novo-ulmi. *G3 (Bethesda)* **5**, 2487–2495, https://doi.org/10.1534/g3.115.021022 (2015).
12. Lengeler, K. B. *et al*. Signal transduction cascades regulating fungal development and virulence. *Microbiology and Molecular Biology Reviews* **64**, 746–785 (2000).
13. Bölker, M. Ustilago maydis a valuable model system for the study of fungal dimorphism and virulence. *Microbiology* **147**, 1395–1401, https://doi.org/10.1099/00221287-147-6-1395 (2001).
14. Edwards, J. A. *et al*. Histoplasma yeast and mycelial transcriptomes reveals pathogenic-phase and lineage-specific gene expression profiles. *BMC Genomics* **14**, 1–19 (2013).
15. Veses, V. & Gow, N. A. Pseudohypha budding patterns of Candida albicans. *Med Mycol* **47**, 268–275, https://doi.org/10.1080/13693780802245474 (2009).
16. Gancedo, J. M. Control of pseudohyphae formation in Saccharomyces cerevisiae. *FEMS Microbioly Reviews* **25**, 107–123 (2001).
17. Khang, C. H. *et al*. Translocation of Magnaporthe oryzae effectors into rice cells and their subsequent cell-to-cell movement. *Plant Cell* **22**, 1388–1403, https://doi.org/10.1105/tpc.109.069666 (2010).
18. Noble, S. M., Gianetti, B. A. & Witchley, J. N. Candida albicans cell-type switching and functional plasticity in the mammalian host. *Nat Rev Microbiol* **15**, 96–108, https://doi.org/10.1038/nrmicro.2016.157 (2017).
19. Couteaudier, Y. & Alabouvette, C. Survival and inoculum potential of conidia and chlamydospores of Fusarium oxysporum f.sp. lini in soil. *Canadian Journal of Microbiology* **36**, 551–556, https://doi.org/10.1139/m90-096 (1990).
20. Lin, X. & Heitman, J. Chlamydospore formation during hyphal growth in Cryptococcus neoformans. *Eukaryot Cell* **4**, 1746–1754, https://doi.org/10.1128/EC.4.10.1746-1754.2005 (2005).
21. McNeel, D. J., Kulkarni, R. K. & Nickerson, K. W. Pleomorphism in Ceratocystis ulmi: chlamydospore formation. *Can J Microbiol* **61**, 1349–1352 (1983).
22. Son, H., Lee, J. & Lee, Y. W. Mannitol induces the conversion of conidia to chlamydospore-like structures that confer enhanced tolerance to heat, drought, and UV in Gibberella zeae. *Microbiol Res* **167**, 608–615, https://doi.org/10.1016/j.micres.2012.04.001 (2012).
23. Miyaji, M., Sano, A. & Sharmin, S. The role of chlamydospores of Paracoccidioides brasiliensis. Japanese. *Journal of Medical Mycology* **44**, 133–138 (2003).
24. Hoes, J. A. Development of chlamydospores in Verticillium nigrescens and Verticillium nubilum. *Canadian Journal of Bonaty* **49**, 1863–1866 (1971).
25. Schade, D., Walther, A. & Wendland, J. The development of a transformation system for the dimorphic plant pathogen Holleya sinecauda based on Ashbya gossypii DNA elements. *Fungal Genetics and Biology* **40**, 65–71, https://doi.org/10.1016/s1087-1845(03)00064-1 (2003).
26. Fones, H. & Gurr, S. The impact of Septoria tritici Blotch disease on wheat: An EU perspective. *Fungal Genet Biol* **79**, 3–7, https://doi.org/10.1016/j.fgb.2015.04.004 (2015).
27. Torriani, S. F. *et al*. Zymoseptoria tritici: A major threat to wheat production, integrated approaches to control. *Fungal Genet Biol* **79**, 8–12, https://doi.org/10.1016/j.fgb.2015.04.010 (2015).
28. Kema, G. H. J. *et al*. Genetic variation for virulence and resistance in the wheat Mycosphaerella graminicola pathosystem I. Interactions between pathogen isolates and host cultivars.PDF. *Phytopathology* **86**, 200–212 (1996).
29. Steinberg, G. Cell biology of Zymoseptoria tritici: Pathogen cell organization and wheat infection. *Fungal Genet Biol* **79**, 17–23, https://doi.org/10.1016/j.fgb.2015.04.002 (2015).
30. King, R. *et al*. A conserved fungal glycosyltransferase facilitates pathogenesis of plants by enabling hyphal growth on solid surfaces. *PLoS Pathog* **13**, e1006672, https://doi.org/10.1371/journal.ppat.1006672 (2017).
31. Motteram, J. *et al*. Aberrant protein N-glycosylation impacts upon infection-related growth transitions of the haploid plant-pathogenic fungus Mycosphaerella graminicola. *Mol Microbiol* **81**, 415–433, https://doi.org/10.1111/j.1365-2958.2011.07701.x (2011).

32. Cousin, A. *et al*. The MAP kinase-encoding gene MgFus3 of the non-appressorium phytopathogen Mycosphaerella graminicola is required for penetration and *in vitro* pycnidia formation. *Mol Plant Pathol* **7**, 269–278, https://doi.org/10.1111/j.1364-3703.2006.00337.x (2006).
33. Mehrabi, R. & Kema, G. H. Protein kinase A subunits of the ascomycete pathogen Mycosphaerella graminicola regulate asexual fructification, filamentation, melanization and osmosensing. *Mol Plant Pathol* **7**, 565–577, https://doi.org/10.1111/j.1364-3703.2006.00361.x (2006).
34. Mehrabi, R., van der Lee, T., Waalwijk, C. & Kema, G. H. MgSlt2, a cellular integrity MAP kinase gene of the fungal wheat pathogen Mycosphaerella graminicola, is dispensable for penetration but essential for invasive growth. *Molecular Plant-Microbe Interactions* **19**, 389–398 (2006).
35. Mehrabi, R., Zwiers, L. H., de Waard, M. A. & Kema, G. H. MgHog1 Rregulates dimorphism and pathogenicity in the fungal wheat pathogen Mycosphaerella graminicola. *Molecular Plant-Microbe Interactions* **19**, 1262–1269 (2006).
36. Mehrabi, R. *et al*. G(alpha) and Gbeta proteins regulate the cyclic AMP pathway that is required for development and pathogenicity of the phytopathogen Mycosphaerella graminicola. *Eukaryot Cell* **8**, 1001–1013, https://doi.org/10.1128/EC.00258-08 (2009).
37. Choi, Y. E. & Goodwin, S. B. Gene encoding a c-Type cyclin in Mycosphaerella graminicola is involved in aerial mycelium formation, filamentous growth, hyphal swelling, melanin biosynthesis, stress response, and pathogenicity. *Molecular Plant-Microbe Interactions* **24**, 469–477 (2011).
38. Gohari, A. M. *et al*. Molecular characterization and functional analyses of ZtWor1, a transcriptional regulator of the fungal wheat pathogen Zymoseptoria tritici. *Mol Plant Pathol* **15**, 394–405, https://doi.org/10.1111/mpp.12102 (2014).
39. Mohammadi, N. *et al*. The ZtVf1 transcription factor regulates development and virulence in the foliar wheat pathogen Zymoseptoria tritici. *Fungal Genet Biol* **109**, 26–35, https://doi.org/10.1016/j.fgb.2017.10.003 (2017).
40. Yemelin, A. *et al*. Identification of factors involved in dimorphism and pathogenicity of Zymoseptoria tritici. *PLoS One* **12**, e0183065, https://doi.org/10.1371/journal.pone.0183065 (2017).
41. Hornby, J. M. *et al*. Inoculum size effect in dimorphic fungi: extracellular control of yeast-mycelium dimorphism in Ceratocystis ulmi. *Applied and Environmental Microbiology* **70**, 1356–1359 (2004).
42. Hornby, J. M. *et al*. Quorum sensing in the dimorphic fungus Candida albicans is mediated by farnesol. *Appl Environ Microbiol* **67**, 2982–2992, https://doi.org/10.1128/AEM.67.7.2982-2992.2001 (2001).
43. Wedge, M. E., Naruzawa, E. S., Nigg, M. & Bernier, L. Diversity in yeast-mycelium dimorphism response of the Dutch Elm disease pathogens: the inoculum size effect. *Can J Microbiol* **62**, 525–529, https://doi.org/10.1139/cjm-2015-0795 (2016).
44. Bottcher, B., Pollath, C., Staib, P., Hube, B. & Brunke, S. Candida species rewired hyphae developmental programs for chlamydospore formation. *Front Microbiol* **7**, 1697, https://doi.org/10.3389/fmicb.2016.01697 (2016).
45. Bago, B. *et al*. Translocation and utilization of fungal storage ipid in the arbuscular mycorrhizal symbiosis. *Plant Physiology* **128**, 108–124 (2002).
46. Fabry, W., Schmid, E. N., Schraps, M. & Ansorg, R. Isolation and purification of chlamydospores of Candida albicans. *Medical Mycology* **41**, 53–58 (2003).
47. Sitton, J. W. & Cook, R. J. Comparative mophology and survival of chlamydospore of Fusarium roseum 'Culmorum' and 'Graminearum'. *Ecology anf Epidemiology* **71**, 85–90 (1981).
48. Palma-Guerrero, J. *et al*. Comparative transcriptome analyses in Zymoseptoria tritici reveal significant differences in gene expression among strains during plant infection. *Mol Plant Microbe Interact* **30**, 231–244, https://doi.org/10.1094/MPMI-07-16-0146-R (2017).
49. Biswas, S., Van Dijck, P. & Datta, A. Environmental sensing and signal transduction pathways regulating morphopathogenic determinants of Candida albicans. *Microbiol Mol Biol Rev* **71**, 348–376, https://doi.org/10.1128/MMBR.00009-06 (2007).
50. Annone, J. In *In: Conferencia regional sobre la septoriosis del trigo* (eds Kohli, M. M. & van Beuningen, L. T.) 80–87 (Mexico: CIMMYT, Montevideo, 1987).
51. Djerbi, M. Epidémiologie du Septoria tritici Rob. et Desm. Conservation et mode de formation de l'inoculum primaire. *Société Française de Phytopathologie*, 91–101 (1977).
52. Quaedvlieg, W. *et al*. Zymoseptoria gen. nov.: a new genus to accommodate Septoria-like species occurring on graminicolous hosts. *Persoonia* **26**, 57–69, https://doi.org/10.3767/003158511X571841 (2011).
53. Jones, D. G. & LEE, N. P. Production of secundary conidia by Septoria tritici in culture. *Transactions British Mycological Society* **62**, 212–213 (1974).
54. Gauthier, G. M. Dimorphism in fungal pathogens of mammals, plants, and insects. *PLoS Pathog* **11**, e1004608, https://doi.org/10.1371/journal.ppat.1004608 (2015).
55. Derridj, S. In *Aerial Plant Surface Microbiology* (eds Morris, C. E., Nicot, P. C. & Nguyen-The, C.) 25–42 (Plenum Press, 1996).
56. Ohm, R. A. *et al*. Diverse lifestyles and strategies of plant pathogenesis encoded in the genomes of eighteen Dothideomycetes fungi. *PLoS Pathog* **8**, e1003037, https://doi.org/10.1371/journal.ppat.1003037 (2012).
57. Fleissner, A. *et al*. The so locus is required for vegetative cell fusion and postfertilization events in Neurospora crassa. *Eukaryot Cell* **4**, 920–930, https://doi.org/10.1128/EC.4.5.920-930.2005 (2005).
58. Glass, N. L., Rasmussen, C., Roca, M. G. & Read, N. D. Hyphal homing, fusion and mycelial interconnectedness. *Trends Microbiol* **12**, 135–141, https://doi.org/10.1016/j.tim.2004.01.007 (2004).
59. Craven, K. D., Velez, H., Cho, Y., Lawrence, C. B. & Mitchell, T. K. Anastomosis is required for virulence of the fungal necrotroph Alternaria brassicicola. *Eukaryot Cell* **7**, 675–683, https://doi.org/10.1128/EC.00423-07 (2008).
60. Prados Rosales, R. C. & Di Pietro, A. Vegetative hyphal fusion is not essential for plant infection by Fusarium oxysporum. *Eukaryotic Cell* **7**, 162, https://doi.org/10.1128/EC.00258-07 (2008).
61. Shetty, N. P. *et al*. Role of hydrogen peroxide during the interaction between the hemibiotrophic fungal pathogen Septoria tritici and wheat. *New Phytol* **174**, 637–647, https://doi.org/10.1111/j.1469-8137.2007.02026.x (2007).
62. Fones, H. & Preston, G. M. Reactive oxygen and oxidative stress tolerance in plant pathogenic Pseudomonas. *FEMS Microbiol Lett* **327**, 1–8, https://doi.org/10.1111/j.1574-6968.2011.02449.x (2012).
63. Yang, C. *et al*. Activation of ethylene signaling pathways enhances disease resiatnce by regulating ROS and phytoalexin production in rice. *The Plant Journal* **89**, 338–353 (2017).
64. Lamb, C. & Dixon, R. A. The oxidative burst in plant disease resistance. *Annual Review of Plant Physiology and Plant Molecular Biology* **48**, 251–275 (1997).
65. Nasution, O. *et al*. Hydrogen peroxide induces hyphal differentiation in Candida albicans. *Eukaryot Cell* **7**, 2008–2011, https://doi.org/10.1128/EC.00105-08 (2008).
66. Levy, E., Eyal, Z. & Hochman, A. Purification and characterization of a catalase-peroxidase from the fungus Septoria tritici. *Archives of Biochemistry and Biophysics* **296**, 321–327 (1992).
67. Morais do Amaral, A., Antoniw, J., Rudd, J. J. & Hammond-Kosack, K. E. Defining the predicted protein secretome of the fungal wheat leaf pathogen Mycosphaerella graminicola. *PLOS ONE* **7**, e49904, https://doi.org/10.1371/journal.pone.0049904 (2012).
68. Lendenmann, M. H., Croll, D., Palma-Guerrero, J., Stewart, E. L. & McDonald, B. A. QTL mapping of temperature sensitivity reveals candidate genes for thermal adaptation and growth morphology in the plant pathogenic fungus Zymoseptoria tritici. *Heredity (Edinb)* **116**, 384–394, https://doi.org/10.1038/hdy.2015.111 (2016).
69. Ponomarenko, A., Goodwin, S. B. & Kema, G. H. Septoria tritici blotch (STB) of wheat. *Plant Health Instructor*, https://doi.org/10.1094/phi-i-2011-0407-01 (2011).

70. Nemecek, J. C., Wüthrich, M. & Klein, B. S. Global control of dimorphism and virulence in fungi. *Science* **312**, 583–588, https://doi.org/10.1126/science.1124105 (2006).
71. Martin, S. W., Douglas, L. M. & Konopka, J. B. Cell cycle dynamics and quorum sensing in Candida albicans chlamydospores are distinct from budding and hyphal growth. *Eukaryot Cell* **4**, 1191–1202, https://doi.org/10.1128/EC.4.7.1191-1202.2005 (2005).
72. Oliveira, R. R., Aguiar, B. M., Tessmann, D. J., Pujade-Renaud, V. & Vida, J. B. Chlamydospores formation by Corynespora cassiicola. *Tropical Plant Pathology* **37**, 415–418 (2012).
73. Coleman, M., Henricot, B., Arnau, J. & Oliver, R. P. Starvation-induced genes of the tomato pathogen Cladosporium fulvum are also induced during growth in planta. *Molecular Plant-Microbe Interactions* **10**, 1106–1109 (1997).
74. Talbot, N. J., Ebbole, D. J. & Hamer, J. E. Identification and characterization of MPG1, a gene involved in pathogenicity from Rice Blast fungus Magnaporthe grisea. *The Plant Cell* **5**, 1575–1590 (1993).
75. Zhan, J. *et al*. Variation for neutral markers is correlated with variation for quantitative traits in the plant pathogenic fungus Mycosphaerella graminicola. *Mol Ecol* **14**, 2683–2693, https://doi.org/10.1111/j.1365-294X.2005.02638.x (2005).
76. Croll, D., Zala, M. & McDonald, B. A. Breakage-fusion-bridge cycles and large insertions contribute to the rapid evolution of accessory chromosomes in a fungal pathogen. *PLoS Genet* **9**, e1003567, https://doi.org/10.1371/journal.pgen.1003567 (2013).
77. Zhan, J., Stefanato, F. L. & McDonald, B. A. Selection for increased cyproconazole tolerance in Mycosphaerella graminicola through local adaptation and in response to host resistance. *Mol Plant Pathol* **7**, 259–268, https://doi.org/10.1111/j.1364-3703.2006.00336.x (2006).
78. Zhan, J. & McDonald, B. A. Thermal adaptation in the fungal pathogen Mycosphaerella graminicola. *Mol Ecol* **20**, 1689–1701, https://doi.org/10.1111/j.1365-294X.2011.05023.x (2011).
79. Kilaru, S. *et al*. A codon-optimized green fluorescent protein for live cell imaging in Zymoseptoria tritici. *Fungal Genet Biol* **79**, 125–131, https://doi.org/10.1016/j.fgb.2015.03.022 (2015).
80. Zala, M. *et al*. Mixed infections alter virulence dynamics and reduce tranmission in the wheat pathogen Zymoseptoria tritici. in submission (2019).
81. Vogel, H. J. A convenient growth medium for Neurospora (medium N). *Microbial Genetics Bulletin* **13**, 42–43 (1956).
82. Meile, L. *et al*. A fungal avirulence factor encoded in a highly plastic genomic region triggers partial resistance to septoria tritici blotch. *New Phytol*, https://doi.org/10.1111/nph.15180 (2018).
83. Schneider, C. A., Rasband, W. S. & Eliceiri, K. W. NIH Image to ImageJ: 25 years of image analysis. *Nature Methods* **9**, 671, https://doi.org/10.1038/nmeth.2089 (2012).
84. Bolger, A. M., Lohse, M. & Usadel, B. Trimmomatic: a flexible trimmer for Illumina sequence data. *Bioinformatics* **30**, 2114–2120, https://doi.org/10.1093/bioinformatics/btu170 (2014).
85. Trapnell, C., Pachter, L. & Salzberg, S. L. TopHat: discovering splice junctions with RNA-Seq. *Bioinformatics* **25**, 1105–1111, https://doi.org/10.1093/bioinformatics/btp120 (2009).
86. Anders, S., Pyl, P. T. & Huber, W. HTSeq–a Python framework to work with high-throughput sequencing data. *Bioinformatics* **31**, 166–169, https://doi.org/10.1093/bioinformatics/btu638 (2015).
87. Robinson, M. D. & Oshlack, A. A scaling normalization method for differential expression analysis of RNA-seq data. *Genome Biology* **11**, 1–9 (2010).
88. Robinson, M. D., McCarthy, D. J. & Smyth, G. K. edgeR: a Bioconductor package for differential expression analysis of digital gene expression data. *Bioinformatics* **26**, 139–140, https://doi.org/10.1093/bioinformatics/btp616 (2010).
89. Oliveros, J. C. V. An interactive tool comparing lists with Venn's diagrams. (2007–2015). http://bioinfogp.cnb.csic.es/tools/venny/index.html.
90. Grandaubert, J., Bhattacharyya, A. & Stukenbrock, E. H. RNA-seq-Based gene annotation and comparative genomics of four fungal grass pathogens in the genus Zymoseptoria identify novel orphan genes and species-specific invasions of transposable elements. *G3 (Bethesda)* **5**, 1323–1333, https://doi.org/10.1534/g3.115.017731 (2015).
91. Plissonneau, C., Hartmann, F. E. & Croll, D. Pangenome analyses of the wheat pathogen Zymoseptoria tritici reveal the structural basis of a highly plastic eukaryotic genome. *BMC Biol* **16**, 5, https://doi.org/10.1186/s12915-017-0457-4 (2018).
92. Wickham, H. *ggplot2: Elegant Graphics for Data Analysis*. 1–212 (Use R. Springer-Verlag, 2009).

Acknowledgements

This study was financed in part by the Coordenação de Aperfeiçoamento de Pessoal de Nível Superior – Brasil (CAPES) – Finance Code 001. We acknowledge Gero Steinberg and Sreedhar Kilaru for generating the fluorescent *Z. tritici* Swiss strains used in this study, and Andrea Sanchez-Vallet for providing the strains. We thank Daniel Croll and Andrea Sanchez-Vallet for critical reading of the manuscript. We also thank Andrea Sanchez-Vallet, Lukas Meile, Julien P. L. Alassimone, and Danilo A. Pereira for discussions in the course of this work. RNA processing and sequencing were performed in the Genetic Diversity Center (GDC) of ETH Zurich and the Genomics Facility of ETH Basel, respectively. Transmission electron microscopy (TEM) and confocal microscopy were performed at the Scientific Center for Optical and Electron Microscopy (ScopeM) of ETH Zurich.

Author Contributions

C.S.F. contributed to the conception and design of the analysis, acquisition of data, analysis of the data, and writing of the original draft of the manuscript. X.M. contributed to the bioinformatic analysis of the RNAseq experiment. M.M.Z. performed experiments to evaluate the stress tolerance of the chlamydospores. B.A.M. acquired funding, contributed to data interpretation, and edited the manuscript. J.P.G. contributed to the conception and design of the analysis, acquisition of data, supervision and editing of the manuscript. All authors read and approved the final manuscript.

Additional Information

Supplementary information accompanies this paper at https://doi.org/10.1038/s41598-019-45994-3.

Competing Interests: The authors declare no competing interests.

Publisher's note: Springer Nature remains neutral with regard to jurisdictional claims in published maps and institutional affiliations.

Open Access This article is licensed under a Creative Commons Attribution 4.0 International License, which permits use, sharing, adaptation, distribution and reproduction in any medium or format, as long as you give appropriate credit to the original author(s) and the source, provide a link to the Creative Commons license, and indicate if changes were made. The images or other third party material in this article are included in the article's Creative Commons license, unless indicated otherwise in a credit line to the material. If material is not included in the article's Creative Commons license and your intended use is not permitted by statutory regulation or exceeds the permitted use, you will need to obtain permission directly from the copyright holder. To view a copy of this license, visit http://creativecommons.org/licenses/by/4.0/.

© The Author(s) 2019